ISSN: 1844-8135 (Print); 2065-2445 (Online)
Research Article

ANNALS OF FOREST RESEARCH
www.afrjournals.org

The Impact of Mineral-solubilizing Microbes on Soil Aggregate Stability through Modulation of Soil Surface Electrochemical Properties

Xuefei Cheng[1,2], Tao Li[2], Hui Nie[1], Yingzhou Tang[1], Xin Liu[1] and Jinchi Zhang[1*]

[1]Co-Innovation Center for Sustainable Forestry in Southern China, Jiangsu Province Key Laboratory of Soil and Water Conservation and Ecological Restoration, Nanjing Forestry University, 159 Longpan Road, Nanjing 210037, China

[2]Department of Renewable Resources, University of Alberta, 442 Earth Sciences Building, Edmonton, Alberta T6G 2E3, Canada

Corresponding Author: Jinchi Zhang, Co-Innovation Center for Sustainable Forestry in Southern China, Jiangsu Province Key Laboratory of Soil and Water Conservation and Ecological Restoration, Nanjing Forestry University, 159 Longpan Road, Nanjing 210037, China, E-mail: zhang8811@njfu.edu.cn

1. Abstract

Purpose: The number of abandoned mines in the world is rapidly increasing, and external soil spray technology has become a common method for their regreening. Due to the unique environmental conditions of rocky waste mining areas, characterized by widespread rocks, externally sprayed soil only acts on the rock surface and is prone to detachment, making it difficult to maintain in the long term. The purpose of this study is to enhance the stability of soil aggregates through the addition of mineral-solubilizing microbes.

Methods: In this study, we simulated the soil microenvironment in the presence of exposed rocks and added microbes that dissolve minerals. Evaluating the effects of soluble microbes on soil aggregate stability from the perspective of soil charge properties and their relationships with soil physicochemical and electrochemical properties.

Results: The results indicated that soil pH, clay content, cation exchange capacity, surface potential and soil surface electric field strength were the key drivers of soil aggregate stability. The addition of microbes reduced soil pH, increased soil cation exchange capacity, and clay content. Structural

equation modeling results showed that soil physicochemical properties ultimately affected soil aggregates through their influence on soil electrochemical properties.

Conclusions: The results suggest that the use of microbes that dissolve minerals could be a viable strategy for the ecological restoration of abandoned mining areas, providing a possible long-term solution for maintaining the efficacy of external soil spray technology. This method addresses the challenges posed by the unique environmental conditions of rocky waste mining areas.

2. Keywords: Soil aggregate stability; Structural equation modeling; Mineral-solubilizing microorganisms; Ecological restoration technique

3. Introduction

Excessive mining activities have led to severe soil erosion, vegetation degradation, and rock exposure in mining areas, causing significant habitat destruction (Eddefli et al. , GUERRA et al. 2017). In recent years, the emerging restoration techniques for abandoned mine slopes, such as external-soil spray seeding, have become essential approaches to address soil and water loss in these areas (O'Donnell et al. 2017, Jiang et al. 2019). In abandoned mining regions, the initial restoration of native ecosystems has been effectively achieved by applying a concoction of grass seeds, soil, and nourishing substances to bare rock surfaces. (Wu et al. 2011, Li et al. 2017). However, due to the unique environmental conditions of rocky waste mining areas, characterized by widespread rocks and thin, infertile soil layers, the widely applied technique of using imported soil for external-soil spray seeding only acts on rock surfaces and is prone to water loss and detachment, making it difficult to maintain in the long term. Research has found that microorganisms play a crucial role in addressing these challenges: rock-dissolving microbial strains can break down rocks into fine particles to form soil (Chaparro et al. 2012, Abd Samad et al. 2017), transforming nutrients in rocks that are difficult for plants to absorb and utilize into bioavailable ionic forms, improving soil physicochemical properties, and promoting plant establishment, ultimately contributing to soil layer thickening in exposed rocky areas (Wu et al. 2017b, Xu et al. 2017, Zhao et al. 2018). This may potentially resolve the issue of hydroseeding matrix efficacy being limited to rock surfaces and prone to detachment. In our previous research, we isolated a series of bacterial, fungal, and actinomycete strains from the soil surrounding weathered limestone

(Wang et al. 2017, Wu et al. 2017b, Wu et al. 2017c, Wang et al. 2018). These microorganisms can secrete various types of acids, acting on rock surfaces to promote rock weathering, thereby reducing particle size and altering soil nutrient content and plant growth characteristics (Prabhakaran et al. 2016, Abd Halin et al. 2017). However, studies on how these microorganisms improve soil structure during external-soil spray seeding restoration processes on exposed cliffs have not yet been conducted.

Evaluating the distribution and steadiness of soil aggregate size serves as one approach to gauge the structural state of the soil (Baumert et al. 2018, Totsche et al. 2018). Studies have shown that the ability of soil to resist mechanical forces from wind, water, and gravity depends on the stability of soil aggregates (Meng et al. 2019, Safar and Whalen 2023). According to previous research findings, the stability of soil aggregates is essentially determined by the combined forces of soil particles (Hu et al. 2015, Ali et al. 2023). Surface charges on particles cause soil colloidal particles to form a strong electrostatic field around them, which not only controls the interactions between charged soil particles (minerals, humus, and microorganisms) but may also govern the interactions between all charged ions and soil particles within the soil (Zhu et al. 2014, Hu et al. 2022).

The interplay among soil particles largely hinges on their electrochemical traits, like Cation Exchange Capacity (CEC), specific surface area (S), and surface charge density (σ_0), which collectively impact the net force applied to soil particles(Hu et al. 2021, Liu et al. 2021).

Previous studies investigating the determinants of soil aggregate stability have predominantly concentrated on elements like maturation effects, differential swelling, the influence of raindrop impact, and physicochemical dispersion (Kinnell 2005) (Kinnell 2005). However, there has been a notable lack of research interpreting soil aggregate stability in light of soil charge characteristics.

Regarding soil charge characteristics, existing studies have demonstrated that the electrochemical attributes of soil particles fluctuate based on alterations in key soil properties. These include the content of Soil Organic Matter (SOM), pH value, and the composition of soil particles (Gruba and Mulder 2015, Liu et al. 2020). Hoper et al. reported a positive correlation between SSA and clay content (Hepper et al.

2006). During the long-term recovery of natural grasslands, CEC and SSA increased with the rise in SOM and clay content (Calero et al. 2017). To accurately and profoundly understand soil and its relationships with numerous micro-processes and macro-phenomena, it is necessary to consider soil surface charge properties. However, the influence of soil charge characteristics on aggregate stability during the hydroseeding revegetation process has not yet been reported. In hydroseeding revegetation, the addition of solubilizing microorganisms will inevitably affect soil properties (Jia et al. 2021). These variations could result in modifications to the electrochemical characteristics of the soil surface, and in turn, influence the stability of soil aggregates.

In this study, we simulated the soil environment of exposed rock slopes during hydroseeding revegetation using indoor pot experiments and investigated the effects of solubilizing microorganism additions on soil stability from the perspective of soil charge characteristics. we aim to test the following hypotheses: the addition of microbial inoculants that enhance rock dissolution will (1) alter the electrochemical properties of the soil; and (2) strengthen soil aggregate stability through changes in soil electrochemical properties. The objective of this work is to demonstrate the impact of adding microbial inoculants that enhance rock dissolution on soil aggregate stability by altering soil electrochemical properties, while also highlighting the role of mineral-solubilizing microorganisms in the restoration of abandoned mining areas.

4. Materials and Methods

4.1 Preparing of experimental materials

The experiment was carried out in the FYS-8 Intelligent Greenhouse at Nanjing Forestry University, which maintained an average temperature of 28°C, a relative humidity of 80%, and a light/dark cycle of 16/8 hours. The maximum photosynthetically active radiation was set at 1800 mol/(m^2·s). Water was added every alternate day at 8:00 AM based on weight measurements, ensuring that each pot had soil water content at 100% of the field water-holding capacity, providing uniform water conditions across pots. *Medicago sativa* (alfalfa) was chosen due to its frequent use in mine ecological restoration (Li et al. 2023). The alfalfa seeds were purchased from Tianhe Nursery Company (Nanjing, Jiangsu, China), following the germination process outlined in previous research (Li et al. 2020) (Table 1).

	MP	NP	MN	CK
NL-1 + NL-11 + NL-15	+	+	-	-
Medicago sativa	+	-	+	-
-: Not added; +: Added; For treatments without microbial inoculants, an equal amount of sterilized microbial liquid culture medium was added. MP: Mineral-solubilizing microbes + plant, NP: plant, MN: Mineral-solubilizing microbes.				

Table 1: Different treatment settings in the pot experiment.

The required microbial inoculants, including the bacteria *Bacillus thuringiensis* (NL-11), the fungus *Gongronella butleri* (NL-15), and the actinomycete *Streptomyces thermophilus* (NL-1), were isolated from the soil surrounding weathered limestone in Nanjing (Wu et al. 2017c). They were applied in a 1:1:1 ratio. In our previous studies, the combined inoculant treatment of NL-1+NL-11+NL-15 showed significant effects on the plant photosynthetic system and root growth (Wu et al. 2017a, Jia et al. 2021). Therefore, this mixed microbial inoculant treatment was chosen to investigate the role of mineral-solubilizing microbes. These microbes were introduced into liquid culture medium and incubated in a shaking flask for 24 hours. Next, the microbial inoculum was moved into a fermenter. Throughout the fermentation process, samples were gathered at specified time intervals to ascertain their OD 600 values (Guimarães et al. 2010). As the curve peaked and started to descend, the microbes were shifted to sterilized plastic bottles for storage in a refrigerator.

To facilitate sampling, this experiment employed non-woven fabric planting bags instead of conventional planting pots, choosing planting bags with a diameter of 35 cm and a height of 25 cm. To simulate the bare rock environment of field spray seeding, exposed limestone blocks were placed at the bottom of the planting bags. The exposed limestone blocks had a diameter of 35 cm and a width of 3 cm, and all blocks used in the experiment were cut from the same exposed rock mining area. The blocks were sourced from Huizhou Craft (Wuxi, Jiangsu, China) and were sanded with 800 grain sandpaper and autoclaved before use.

Soil was collected from the Xiashu Forestry Station, located at 32°7'47" N latitude and 119°13'15" E longitude. Soil from nearby carbonate rock mining areas was used as a recipient soil for the restoration efforts. According to the United States Department of Agriculture soil taxonomy, the soil was classified as an Ultisol, with a loam texture (Staff 2014). The soil pH was 7.15 (soil-to-water ratio of 1:5), and the concentrations of available potassium and available phosphorus were 100.25 mg/kg and 9.89 mg/kg, respectively (Wang et al. 2019). Prior to the pot experiment, the soil was sieved with a 5 mm mesh and sterilized to ensure no other microbes were present in the soil before adding the mixed microbial inoculant.

4.2. Experimental design

Before the experiment, each pot was filled with 8 kg of soil and 96 mL of mixed microbial inoculant (based on the optimal ratio obtained from previous research, which is 60 mL of microbial inoculant per 5 kg of soil (Li et al. 2021)). Microbial inoculation treatments included: NL-1 + NL-11 + NL-15, and sterilized microbial liquid culture medium (control check, CK). The experiment consisted of four treatment groups, as follows:

When adding the microbial inoculants, the exposed rocks were first placed at the bottom of the planting bags. Next, the microbial inoculants were mixed with a portion of the soil and placed on the exposed rocks to ensure full contact between the rock-dissolving microbes and the rock surface. Finally, the germinated seeds were transplanted.

Each treatment group had 12 replicates, totaling 48 pots. During sampling, the non-woven fabric planting bags were cut open, and soil samples were collected from the bottom up. First, soil samples adhering to the exposed rock surface were collected, followed by layered collection of soil samples from 0-1 cm, 3-5 cm, and 6-8 cm (distances represent the distance from the exposed rock surface). This was done to evaluate the effects of solubilizing microbes at the rock-soil interface.

The potted plants were cultivated in the greenhouse from December 2021 to May 2022. In May2022,

soil samples were extracted for subsequent soil parameter measurements.

4.3. Basic soil properties

The soil particle size distribution was gauged using a laser particle size analyzer (Malvern Mastersizer 2000, Shanghai, China), following the method outlined by Wei et al. (Wei et al. 2018). The soil's pH was ascertained with a pH electrode (ST3100, Ohaus, China) using a 1:2.5 soil-to-water ratio. We estimated the soil's Total Nitrogen (TN) using an elemental analyzer (Vario MAX cube; Elementar, Germany), while Soil Organic Carbon (SOC) was quantified via the potassium dichromate oxidation external heating method (HJ615-2011). Soil Cation Exchange Capacity (CEC) was determined using the cobalt chloride-ammonia method (HJ 889-2017). Soil calcium carbonate content (CaCO3) was measured using the gas volumetric method.

4.4 Soil surface electrochemical properties

Soil surface electrochemical properties were determined using the combined determination method (Liu et al. 2013). In brief, the soil samples were first saturated with H^+ ions, followed by exchange with a mixed solution of NaOH and Ca $(OH)_2$. Finally, the concentrations of Na^+ and Ca^{2+} in the supernatant were measured, and E_0, S, and σ_0 (Ma et al. 2023) were calculated based on the double-layer theory. Calculate the soil surface electrochemical properties of the soil samples using the following equations (Li et al. 2011, Liu et al. 2013, Liu et al. 2022).

Surface potential φ_0:

$$\varphi_0 = \frac{2RT}{2(\beta_{Ca} - \beta_{Na})F} ln \frac{a^0{}_{Ca} N_{Na}}{a^0_{Na} N_{Ca}}$$

In the formula, φ_0 represents the surface potential in volts (V); R is the ideal gas constant in J mol^{-1} K^{-1}; T is the absolute temperature; F is the Faraday constant in C mol^{-1}; β_{Ca} and β_{Na} are the effective charge coefficients for Ca^{2+} and Na^+ ions, respectively, with β_{Ca}=-0.0213In($I^{0.5}$)+1.2331 and β_{Na}=0.0213In($I^{0.5}$)+0.766; I is the ionic strength in mol L^{-1}; a^0_{Na} and $a^0{}_{Ca}$ are the activities of Na^+ and Ca^{2+} in the solution in mol mol /L^{-1}; N_{Na} and N_{Ca} are the adsorbed amounts of Na^+ and Ca^{2+} in the soil in mol /g^{-1}.

Surface charge density σ_0:

$$\sigma_0 = \mathrm{sgn}(\varphi_0)\sqrt{\frac{\varepsilon RT(a^{0Na}e^{\frac{\beta_{\mathrm{Na}}F\varphi_0}{RT}} + a^0_{\mathrm{Ca}}\mathrm{e}^{\frac{2\beta_{\mathrm{Ca}}F\varphi_0}{RT}})}{2\pi}}$$

In the formula, φ_0 represents the surface charge density of charged soil particles, in c m^{-2}; ε is the dielectric constant (in water, its value is 8.9×10^{-10}), in C^2 J^{-1} dm^{-1}.

Surface electric field strength E_0:

$$E_0=\frac{4\pi}{\varepsilon}\sigma_0$$

In the formula, E_0 represents the surface electric field strength, in V m^{-1}.

Specific surface area S:

$$S = \frac{N_{\mathrm{Na}}K}{ma^0_{Na}}e^{\frac{\beta_{\mathrm{Nu}}F\varphi_0}{2RT}} = \frac{N_{\mathrm{Ca}}K}{ma^0_{Ca}}e^{\frac{\beta_{Ca}F\varphi_0}{RT}}$$

In the formula, S represents the specific surface area, in m^2 g^{-1}; m =0.5259ln (c^0_{Na}/ c^0_{Ca})+1.992, where c^0_{Na} and c^0_{Ca} are the concentrations of Na^+ and Ca^{2+} in the bulk solution, respectively.

κ is the Debye parameter, in 1 dm^{-1}, and its reciprocal κ^{-1} represents the thickness of the diffuse double layer of colloidal particles. Its value can be expressed as:

$$\kappa=\sqrt{\frac{8\pi F^2 I}{\varepsilon RT}}$$

Surface charge quantity SCN:

$$SCN=10^5\frac{S\sigma_0}{F}$$

In the formula, SCN represents the surface charge quantity, in cmol kg^{-1}.

4.5. Determination of soil aggregate stability

Wet sieving was performed following the method of Elliot (Elliott 1986) . The calculation formulas for various soil aggregate indices are as follows:

The calculation formula for large aggregate proportion ($R_{0.25}$) is:

$$\mathrm{R}_{0.25} = \frac{M_{\mathrm{r}} > 0.25}{M_{\mathrm{T}}} \times 100\% = (1 - \frac{M_{\mathrm{r}} < 0.25}{M_{\mathrm{T}}}) \times 100\%$$

In the formula: M_{r} is the weight of aggregates of each particle size (g), and M_{T} is the total weight of aggregates (g).

The calculation formulas for the mean weight diameter (MWD, mm) and geometric mean diameter

(GMD, mm) are:

$$\text{MWD}=\sum_{i}^{n} x_i w_i \,/\, \sum_{i}^{n} w_i$$

$$\text{GMD}=exp(\sum_{i}^{n} w_i ln x_i \,/\, \sum_{i}^{n} w_i)$$

In the formula: x_i is the average diameter of soil particle size (mm), and w_i is the proportion of aggregates of different soil particle sizes to the total aggregates.

The calculation formula for soil aggregate fractal dimension is:

$$W/W_{\mathrm{T}} = (\bar{R}_i/R_{\max})^{3-D}$$

Taking the base 10 logarithm on both sides: ：

$$\lg W/W_{\mathrm{T}} = (3-D)\lg(\bar{R}i/R_{max})$$

In the formula: $D$is the fractal dimension of the distribution of soil water-stable aggregates of various particle sizes, W is the cumulative mass of particle sizes smaller than R_i, $W_T$is the total mass, $\bar{R}i$ is the average value between two adjacent particle sizes R_i and R_{i+1}, and $R_{max}$is the average diameter of the maximum particle size.

4.6. Statistical analysis

Data analysis was performed using Microsoft Excel 2010 and the SPSS software package (version 21.0, IBM, Armonk, NY, USA). The data were presented as mean ± Standard Deviation (SE). We analyzed the normality and homogeneity of the data and confirmed that they met the assumptions of normality and homogeneity. The impact of varying treatments on different indicators was assessed via analysis of variance (ANOVA) coupled with Duncan's test, with a significance level set at $p < 0.05$. All histograms were fitted using Origin2022 software.

Redundancy Discriminant Analysis (RDA) was performed using Canoco 5.0 (Microcomputer Power, Ithaca, NY, USA) to reveal the relationships between soil aggregate stability characteristics, physicochemical properties, and soil electrochemical properties. Each arrow, typically denoting a numeric variable, points towards the direction of the most rapid growth of environmental variable

values. The angle (alpha) between arrows signifies the correlation between environmental variables: acute angles represent positive correlation, while angles larger than 90 degrees indicate negative correlation. The length of the arrow signifies the degree of fit of the indicator. The length of the arrow represents the degree of fit of the indicator. Structural Equation Modeling (SEM) was used to study the effects of soil characteristics and soil electrochemical properties on soil aggregates. SEM analysis was performed using AMOS 24.0 (SPSS Inc., Chicago, IL, USA).

5. Results

5.1. Soil properties

The soil chemical properties showed significant differences among different treatments ($p < 0.05$). The lowest values of CaCO3, C/N, and SOC were found in the CK control group. The highest value of CaCO3 (117.68 g kg^{-1}), CEC (11.72 c mol kg^{-1}), and SOC (0.55 g kg^{-1}) were observed in the MP treatment, where the soil was closest to the bare rocks. The lowest pH value (5.77) was found in the MN treatment, which was 15.14% lower than the pH value (6.80) in the CK control (Table 2).

	Soil depth (cm)	**$CaCO_3$ (g kg^{-1})**	**SOC (g kg^{-1})**	**N (g kg^{-1})**	**C/N**	**pH**	**CEC (c mol kg^{-1})**
MP	0-1	112.68 ± 0.05Bb	0.55 ± 0.10Aa	0.03 ± 0.01Aa	18.00 ± 6.73Aa	5.99 ± 0.25Aa	11.72 ± 0.11ABa
	3-5	111.89 ± 0.05Ba	0.44 ± 0.08Aab	0.04 ± 0.01Aa	14.08 ± 0.38Aa	5.95 ± 0.18ABa	11.12 ± 0.01Ab
	6-8	103.15 ± 0.10Aa	0.30 ± 0.04Bb	0.03 ± 0.01Ca	17.56 ± 2.36Aa	6.22 ± 0.22Ba	10.80 ± 0.39Ab
NP	0-1	113.55 ± 0.02Bc	0.20 ± 0.06Bb	0.03 ± 0.01Ab	18.22 ± 1.84Aa	6.15 ± 0.14Aa	10.9 ± 0.79Ba
	3-5	104.19 ± 0.02Bb	0.40 ± 0.03Aa	0.04 ± 0.01Aab	13.60 ± 3.86Abb	6.20 ± 0.07Bb	10.73 ± 0.22Aa
	6-8	116.08 ± 0.08Aa	0.43 ± 0.09Aa	0.05 ± 0.01Ba	13.58 ± 1.94Aab	6.12 ± 0.05Bb	11.14 ± 0.46Aa
MN	0-1	115.15 ± 0.16Aa	0.23 ± 0.09ABa	0.04 ± 0.01Ab	14.33 ± 2.32Aa	5.77 ± 0.03Aab	12.08 ± 0.31Aa
	3-5	113.71 ± 0.04Aa	0.19 ± 0.01Bb	0.06 ± 0.01Ba	8.94 ± 0.95Ba	5.95 ± 0.16ABb	11.12 ± 1.06Aa
	6-8	101.31 ± 0.25Aa	0.17 ± 0.02Cb	0.06 ± 0.01Aa	7.99 ± 0.78Ba	6.01 ± 0.43ABa	11.83 ± 0.50Aa
CK	0-1	76.17 ± 0.08Aa	0.28 ± 0.17Ba	0.04 ± 0.01Ab	12.78 ± 3.67Aa	6.37 ± 0.17Bb	9.99 ± 0.37Cab

	3-5	84.63 ± 0.02Aa	0.23 ± 0.11Ba	0.05 ± 0.01Ba	9.71 ± 1.21Ba	6.80 ± 0.13Bb	9.58 ± 0.41Bb
	6-8	77.89 ± 0.11Aa	0.16 ± 0.10Ca	0.05 ±0.01ABab	9.64 ± 1.17Ba	6.65 ± 0.14Ba	11.19 ± 0.89Aa

mean ± SE, n = 4, SE denotes the standard error. Lowercase letters represent significant differences among different soil layers within the same treatment ($p < 0.05$); uppercase letters represent significant differences among different treatments within the same soil layer ($p < 0.05$). $CaCO_3$ - soil calcium carbonate content, SOC - soil organic carbon, N - Total nitrogen, CEC - cation exchange capacity. MP: Mineral-solubilizing microbes + plant, NP: plant, MN: Mineral-solubilizing microbes.

Table 2: Chemical properties of testing soil in different treatments.

A significant difference ($p<0.05$) in clay content was observed between the treatment groups and the CK control group, while sand and silt content showed no significant differences among the different treatments and the CK control (Figure 1).

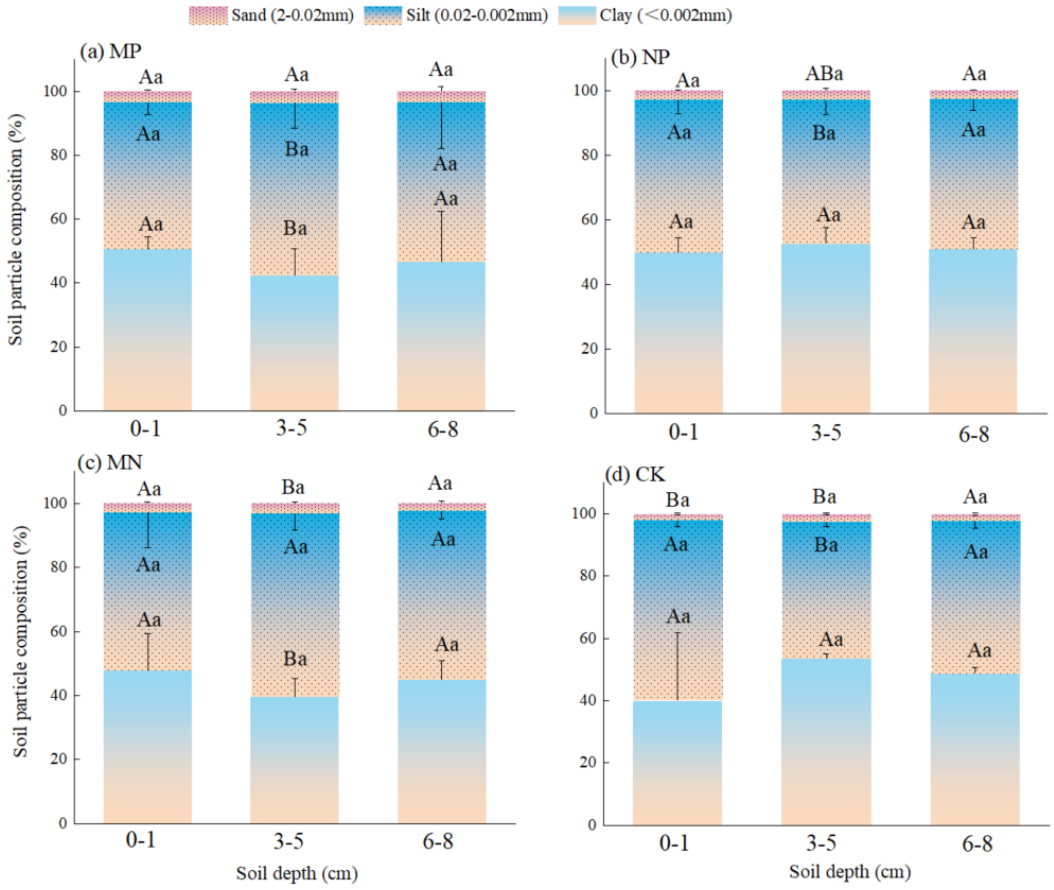

Figure 1: Soil particle composition of different treatments (mean ± SE, n = 4), SE denotes the standard error. Lowercase letters represent significant differences among different soil layers within the same treatment ($p < 0.05$); uppercase letters represent significant differences among different treatments within the same soil layer ($p < 0.05$). (a): MP: Mineral-solubilizing microbes + plant, (b): NP: plant, (c)

MN: Mineral-solubilizing microbes, (d) CK.

5.2 Ion exchange equilibrium results and surface electrochemical properties of soil samples

Following the principles of surface parameter measurement proposed by Li et al. (Li et al. 2011), the calculation results are presented in Table 3. The addition of rock-solubilizing microbial inoculums significantly increased the equilibrium activity and concentration of calcium and sodium ions ($p < 0.05$). Compared to the treatment with plants only (NP), the addition of Rock-Solubilizing Microbial Inoculums significantly increased the number of sodium and calcium ions in the diffusion layer (Table 3).

	Soil depth (cm)	a^0_{Ca} (m mol L^{-1})	a^0_{Na} (m mol L^{-1})	c^0_{Ca} (m mol L^{-1})	c^0_{Na} (m mol L^{-1})	m	N_{Ca} (10^{-5}mol g^{-1})	N_{Na} (10^{-5}mol g^{-1})
MP	0-1	1.18 ± 0.05Aa	5.63 ± 0.32Aa	1.59 ± 0.05Aa	6.47 ± 0.40Aa	2.76 ± 0.06Bb	6.44 ± 0.13Aa	1.81 ± 0.00Aa
	3-5	0.92 ± 0.10ABb	5.31 ± 0.10Aa	1.22 ± 0.14Bb	6.10 ± 0.15Aa	2.88 ± 0.04Aba	6.62 ± 0.13Aa	1.31 ± 0.14Ab
	6-8	0.49 ± 0.03Cc	2.73 ± 0.34Cb	0.60 ± 0.05Cc	3.31 ± 0.36Bb	2.86 ± 0.01Ba	4.57 ± 1.21Abb	1.09 ± 0.06Ac
NP	0-1	0.99 ± 0.03Bb	4.86 ± 0.16Ba	1.29 ± 0.04Bb	5.81 ± 0.28Ba	2.73 ± 0.05Bc	6.22 ± 0.01Ba	1.20 ± 0.17Ba
	3-5	1.11 ± 0.03Aa	5.55 ± 0.82Aa	1.39 ± 0.05Ba	6.21 ± 0.87Aa	2.91 ± 0.03Ab	5.23 ± 0.35Bb	0.96 ± 0.14Ba
	6-8	0.74 ± 0.05Bc	3.64 ± 0.25Bb	0.90 ± 0.06Bc	4.11 ± 0.17Ab	3.10 ± 0.03Aa	5.01 ± 0.26Ab	0.97 ± 0.13ABa
MN	0-1	0.94 ± 0.04Ba	3.70 ± 0.15Cb	1.23 ± 0.03Ba	4.28 ± 0.12Cb	2.56 ± 0.08Cb	5.56 ± 0.30Ca	1.23 ± 0.12Ba
	3-5	0.86 ± 0.14Ba	4.32 ± 0.40Bb	1.10 ± 0.18Aa	4.91 ± 0.36Ba	2.80 ± 0.09Ba	5.24 ± 0.24Bab	1.06 ± 0.21ABa

	6-8	0.89 ± 0.09Aa	4.22 ± 0.22Aa	1.14 ± 0.12Aa	4.80 ± 0.17Aab	2.82 ± 0.01Ca	4.99 ± 0.05Ab	1.04 ± 0.10Aa
CK	0-1	0.47 ± 0.01Cb	3.30 ± 0.18Ca	0.64 ± 0.03Cb	4.24 ± 0.20Ca	2.94 ± 0.04Aa	4.34 ± 0.39Da	0.73 ± 0.01Cb
	3-5	0.63 ± 0.06Ca	3.43 ± 0.20Ba	0.87 ± 0.05Ca	4.16 ± 0.21Ca	2.84 ± 0.03Abb	4.15 ± 0.04Ca	0.95 ± 0.05Ba
	6-8	0.54 ± 0.05Ba	3.02 ± 0.43BCb	0.78 ± 0.07Cb	3.59 ± 0.39Ba	2.72 ± 0.02Dc	3.44 ± 0.16Bb	0.81 ± 0.07Ba

mean ± SE, n = 4, SE denotes the standard error. Lowercase letters represent significant differences among different soil layers within the same treatment ($p < 0.05$); uppercase letters represent significant differences among different treatments within the same soil layer ($p < 0.05$). MP: Mineral-solubilizing microbes + plant, NP: plant, MN: Mineral-solubilizing microbes.

a^0_{Ca}: Ca^{2+} equilibrium activity, a^0_{Na}: Na^+ equilibrium activity, c^0_{Ca}: Ca^{2+} equilibrium concentration, c^0_{Na}: Na^+ equilibrium concentration, N_{Ca}: Ca^{2+} diffusion layer ion quantity, N_{Na}: Na^+ diffusion layer ion quantity.

Table 3: Calculation results of ion exchange equilibrium of soils.

The electrochemical properties of soil particle surfaces varied among different treatments. For SCN, E_0, and S, the highest average values were found in the MP treatment, where the soil was closest to the rocks (Table 4). Moreover, the values decreased as the distance from the rocks increased. The soil particle charge quantity and specific surface area in the CK control was significantly lower than those in the treatments ($p<0.05$).

	Soil depth (cm)	***SCN*** **(c mol kg^{-1})**	***S*** **(m^2 g^{-1})**	***σ₀*** **(c g^{-2})**	***E₀*** **(108 V m^{-1})**	***φ₀*** **(mV)**
MP	0-1	15.07 ± 0.1Aa	61.01 ± 0.47Aa	0.24 ± 0.01Aa	3.44 ± 0.08Aa	-117.63 ± 0.40Ca
	3-5	10.41 ± 0.94Ab	43.26 ± 6.19ABb	0.23 ± 0.01Aa	3.48 ± 0.08Aa	-115.44 ± 2.93Ca
	6-8	5.72 ± 0.76Cc	29.16 ± 1.57Bc	0.19 ± 0.01Cb	2.31 ± 0.19Bb	-116.75 ± 0.89Da
NP	0-1	11.70 ± 0.53Ba	48.34 ± 2.07Ba	0.22 ± 0.01Ba	3.14 ± 0.13Ba	-115.33 ± 2.55Ca
	3-5	10.70 ± 1.03Aa	46.31 ± 3.71Aa	0.24 ± 0.01Aa	3.33 ± 0.08ABa	-117.40 ± 1.55Ca

	6-8	9.15 ± 0.27Ab	28.26 ± 4.84Bb	0.22 ± 0.01Aa	3.22 ± 0.11Aa	-113.14 ± 2.30Ca
MN	0-1	10.61 ± 0.59Ca	42.85 ± 0.58Ca	0.20 ± 0.00BCb	2.88 ± 0.12Cb	-108.39 ± 2.22Bb
	3-5	9.29 ± 1.03ABab	40.24 ± 4.85ABa	0.22 ± 0.00Aab	3.16 ± 0.05Bab	-109.26 ± 0.56Bb
	6-8	9.17 ± 0.14Ab	38.44 ± 2.44Aa	0.21 ± 0.01ABb	2.99 ± 0.16Aa	-104.55 ± 0.24Ba
CK	0-1	6.58 ± 0.05Db	28.31 ± 0.69Db	0.19 ± 0.01Ca	2.25 ± 0.05Db	-97.65 ± 0.44Aa
	3-5	7.99 ± 0.38Ba	34.57 ± 3.22Bab	0.19 ± 0.01Ba	2.79 ± 0.16Ca	-101.29 ± 0.03Ab
	6-8	6.59 ± 0.06Bb	31.42 ± 1.16Ba	0.19 ± 0.01BCa	2.28 ± 0.24Bb	-98.48 ± 0.49Ac

mean ± SE, n = 4, SE denotes the standard error. Lowercase letters represent significant differences among different soil layers within the same treatment ($p < 0.05$); uppercase letters represent significant differences among different treatments within the same soil layer ($p < 0.05$). *SCN* - surface charge quantity, *S* - specific surface area, σ_0 - surface charge density, E_0 - surface electric field strength, φ_0 - surface potential. MP: Mineral-solubilizing microbes + plant, NP: plant, MN: Mineral-solubilizing microbes.

Table 4: Soil surface electrochemical properties.

5.3 Soil aggregate stability

Figure 2 displays the distribution of soil aggregate sizes determined through wet sieving. Across all treatments, water-stable aggregates with varied particle sizes were more abundant in the 0.25-0.106 mm range, followed by the 0.106-0.053 mm range, and the least numerous in the >2 mm range. The percentage of aggregates within the 0.106-0.053 mm range in the CK control significantly outpaced that in the treatments ($p < 0.05$), standing 45.12% and 35.01% higher than MN and NP, respectively. The integration of rock-dissolving microbial inoculums notably enhanced the percentage of aggregates in the 1-0.5 mm and 0.5-0.25 mm ranges (Figure 2).

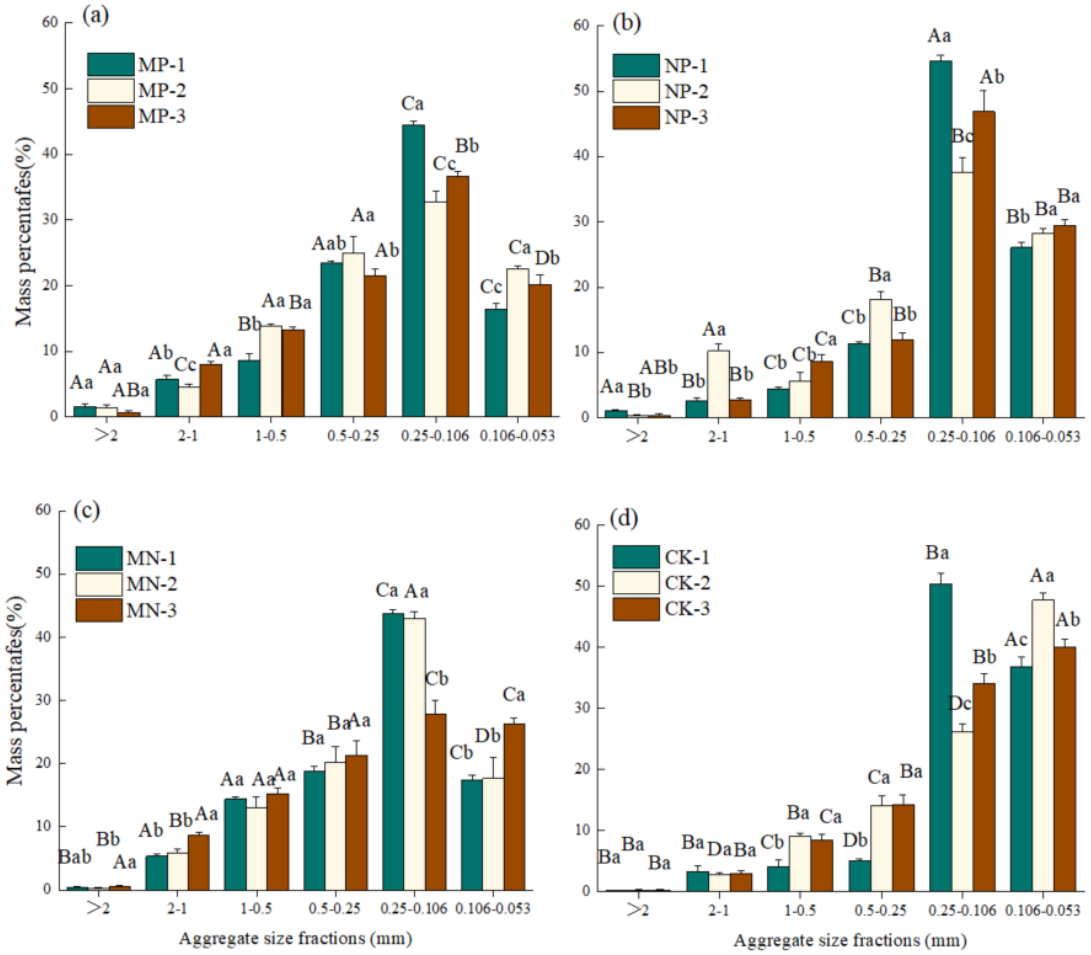

Figure 2: Soil aggregate size distribution under different treatments. mean ± SE, n = 4, SE denotes the standard error. Lowercase letters represent significant differences among different soil layers within the same treatment ($p < 0.05$); uppercase letters represent significant differences among different treatments within the same soil layer ($p < 0.05$). MP: Mineral-solubilizing microbes + plant, NP: plant, MN: Mineral-solubilizing microbes.

Table 5 presents the water stability characteristics of soil aggregates under different treatments. The values of R0.25 and MWD showed similar variations among the four treatments, with the lowest values observed in the CK control, and the highest values found in the MP treatment, where the soil was closest to the rocks, with significant differences ($p < 0.05$). However, D exhibited a different trend, with the highest value in the CK control.

	Soil depth (cm)	$R_{0.25}$/%	MWD/mm	GMD/mm	D
MP	0-1	24.52 ± 0.009Aa	0.272 ± 0.002Aa	0.166 ± 0.000Aa	2.792 ± 0.006Db
	3-5	19.65 ± 0.013Ab	0.251 ± 0.010Ab	0.160 ± 0.002Aa	2.807 ± 0.005Da
	6-8	21.8 ± 0.006Ac	0.261 ± 0.008Aab	0.166 ± 0.005Aa	2.809 ± 0.009Ca
NP	0-1	8.04 ± 0.008Cc	0.169 ± 0.007Cb	0.114 ± 0.002Cb	2.900 ± 0.003Ba
	3-5	16.13 ± 0.008Ba	0.237 ± 0.008Aa	0.141 ± 0.003Ba	2.860 ± 0.009Bc
	6-8	11.69 ± 0.015Cb	0.173 ± 0.012Bb	0.118 ± 0.004Cb	2.908 ± 0.011Ab
MN	0-1	20.09 ± 0.003Ba	0.235 ± 0.006Ba	0.157 ± 0.002Ba	2.833 ± 0.004Ca
	3-5	19.15 ± 0.018Aa	0.235 ± 0.012Aa	0.157 ± 0.009Aa	2.832 ± 0.014Ca
	6-8	15.78 ± 0.004Bb	0.244 ± 0.013Aa	0.157 ± 0.004Ba	2.840 ± 0.001Ba
CK	0-1	7.69 ± 0.002Cb	0.144 ± 0.004Db	0.099 ± 0.001Dc	2.952 ± 0.002Aa
	3-5	12.07 ± 0.003Ca	0.165 ± 0.005Ba	0.106 ± 0.002Cb	2.898 ± 0.005Ab
	6-8	11.60 ± 0.012Ca	0.170 ± 0.005Ba	0.111 ± 0.002Ca	2.920 ± 0.008Ab

mean ± SE, n = 4, SE denotes the standard error. Lowercase letters represent significant differences among different soil layers within the same treatment ($p < 0.05$); uppercase letters represent significant differences among different treatments within the same soil layer ($p < 0.05$). MP: Mineral-solubilizing microbes + plant, NP: plant, MN: Mineral-solubilizing microbes. MWD: mean weight diameter, GMD: geometric mean diameter, D: fractal dimension of the distribution of soil water-stable aggregates of various particle sizes.

Table 5: Soil aggregate stability characteristics under different treatments.

5.4 Linking soil physicochemical properties, soil electrochemical properties, and S soil aggregate stability characteristics

The RDA was conducted on soil physicochemical properties, soil surface charge properties, and soil aggregate stability characteristics (Figure 3). From the figure, it can be seen that Axis 1 and Axis 2 explained 67.82% and 1.49% of the total variation, respectively. There was a positive correlation between pH and φ_0. Electrochemical property indicators were significantly positively correlated with CEC, Clay, and C/N, and also exhibited a strong correlation with soil aggregate stability indices. Based

on the RDA results, we selected soil characteristic indicators CEC, pH, Clay, and C/N, along with soil electrochemical properties E_0 and φ_0, to be used in the equation model with soil fractal dimensions.

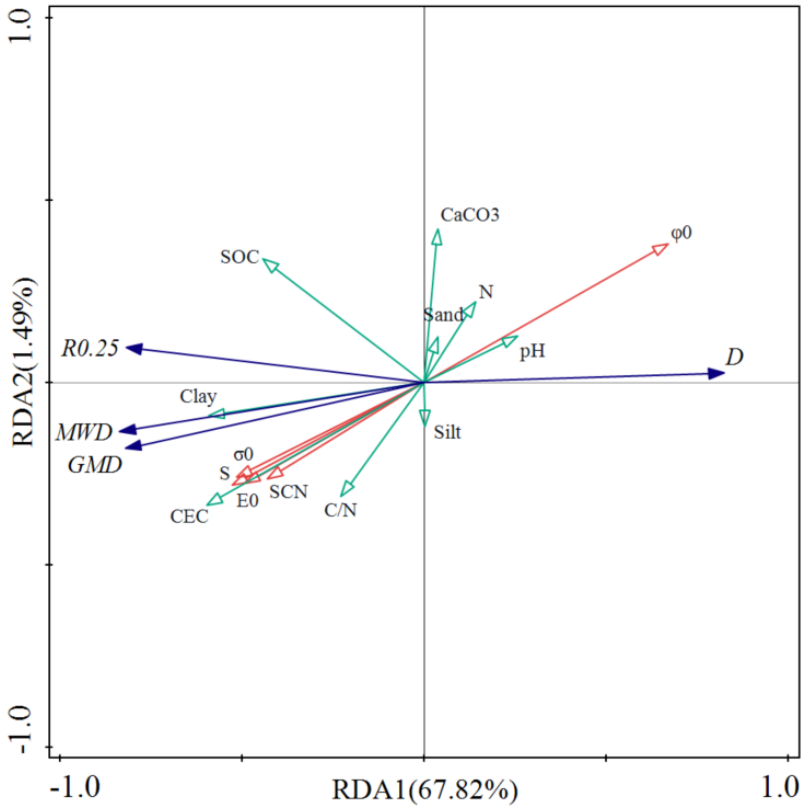

Figure 3: Redundancy analysis (RDA) of soil aggregate stability characteristics with soil physicochemical properties and soil electrochemical properties. $CaCO_3$ - soil calcium carbonate content, SOC - soil organic carbon, C/N – Total carbon / Total nitrogen, N – Total nitrogen, CEC - cation exchange capacity. *SCN* - surface charge quantity, *S* - specific surface area, σ_0 - surface charge density, E_0 - surface electric field strength, φ_0 - surface potential. MWD: mean weight diameter, GMD: geometric mean diameter, D: fractal dimension of the distribution of soil water-stable aggregates of various particle sizes.

5.5 SEM Results

To evaluate the direct and indirect effects of soil physicochemical properties and soil electrochemical properties on soil aggregate stability, the fractal dimensions were used to determine aggregate stability. Since a larger soil fractal dimension indicates poorer soil aggregate stability, the negative correlation of

different parameters with D signifies a positive influence on soil aggregate stability. According to the results of the structural equation model (Figure 4a), C/N, CEC, Clay, σ_0, and E_0 had direct effects on D, while the remaining indicators indirectly influenced D. CEC and Clay were found to be significantly negatively correlated with D, with correlation coefficients of -0.372 ($p<0.01$) and -0.344 ($p<0.05$), respectively.

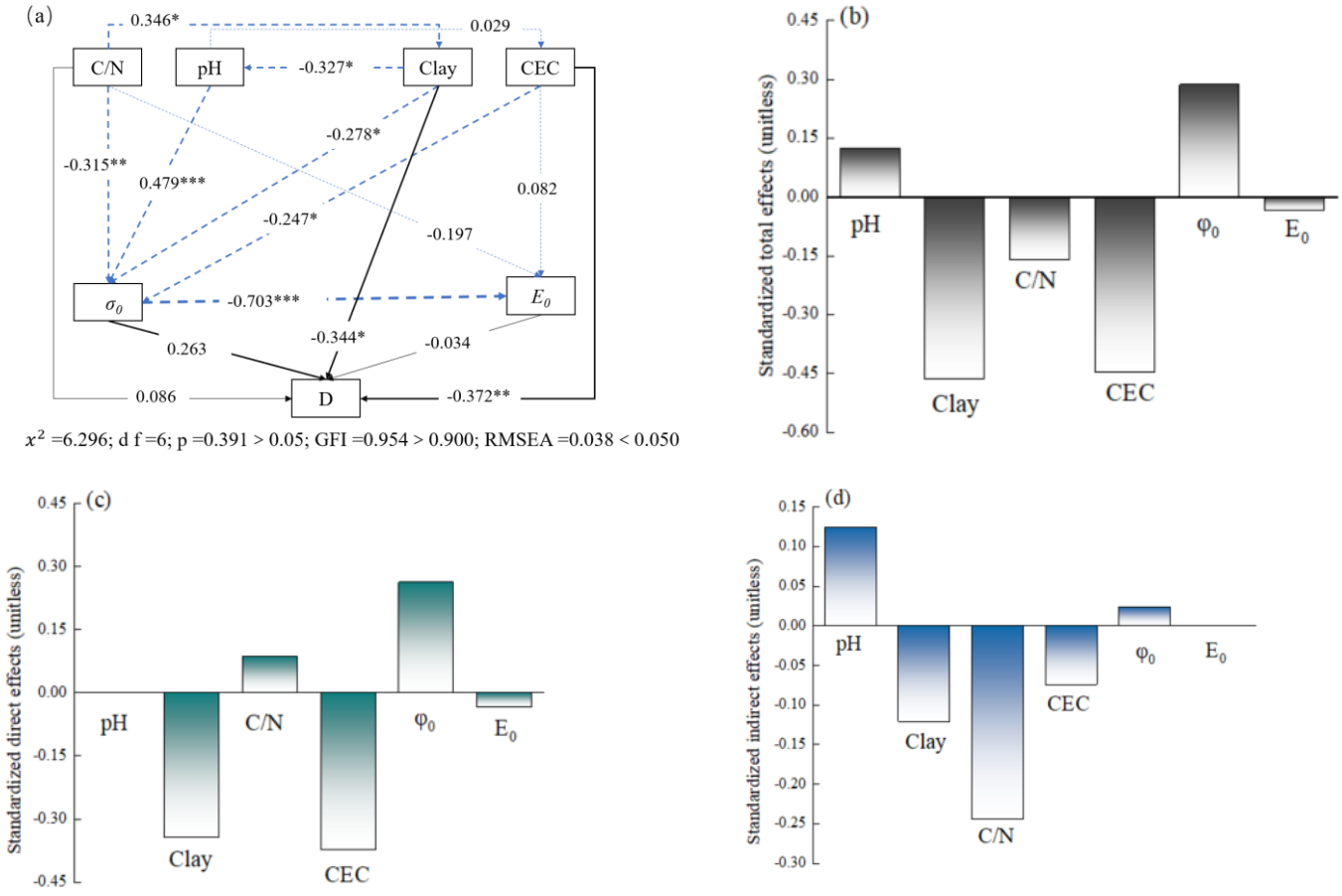

Figure 4: Structural equation model of the effects of soil characteristics and soil electrochemical properties on soil aggregate stability. Boxes show variables included in the model. Test results of the goodness of model fit: Chi-square ($\chi 2$) = 6.296, p value = 0.391 > 0.05, goodness-of-fit index (GFI) = 0.954 > 0.9, root square mean error of approximation (RMSEA) = 0.038 < 0.05. * indicates a significant correlation at $p < 0.05$, ** indicates a significant correlation at $p < 0.01$, and *** indicates a significant correlation at $p < 0.001$. The solid line represents the path that directly affects soil aggregate

fractal dimension, and the dashed line represents the path that indirectly affects soil aggregate fractal dimension. Numbers on arrows are standardized path coefficients. Widths of arrows represent the strength of the relationships. (b): Standardized total effects (direct plus indirect effects) derived from the structural equation models depicted above. (c): Standardized direct effects derived from the structural equation models depicted above. (d): Standardized indirect effects derived from the structural equation models depicted above. C/N – Total carbon / Total nitrogen, CEC - cation exchange capacity. φ_0 - surface potential, E_0 - surface electric field strength, D - soil aggregate fractal dimension.

To gain a deeper understanding of the direct and indirect impacts of various driving factors on soil aggregate stability, we analyzed the standardized impact coefficients of different parameters. The standardized total impact coefficients, as displayed in Figure 4b, revealed that CEC and Clay exerted the most substantial positive influences on soil aggregate stability, with respective values of 0.446 and 0.464. Conversely, pH affected soil aggregate stability indirectly only, as depicted in Figure 4d, with a value of 0.125.

6. Discussion

In the current research, we explored the implications of utilizing rock-dissolving microbial inoculants on soil aggregate stability and associated soil characteristics. Our results demonstrated a notable elevation in Soil Organic Carbon (SOC) and Cation Exchange Capacity (CEC) following the application of rock-dissolving microbial inoculants (Table 2). A significant difference in clay content was found between the treatment and CK control, which is consistent with previous research that emphasized the importance of soil clay content in enhancing soil structure and stability (Khan et al. 2009). Increased CEC indicates an improved capacity for soil to retain and exchange nutrients, which is crucial for maintaining soil fertility and promoting plant growth (Iturri and Buschiazzo 2014). Additionally, SOC is widely recognized for its role in enhancing soil aggregate stability as a binding agent, promoting microbial activity, and increasing nutrient availability.

The results were in line with previous research demonstrating that rock-dissolving microbial inoculants promote rock dissolution by secreting organic acids (Wu et al. 2017b, Li et al. 2020). The decrease in

pH values affects the ionization state of soil particle surface functional groups, subsequently controlling the number of charged sites (Rengasamy and Olsson 1991). This process helps regulate protonation and deprotonation reactions of variable charge sites, the valence of exchangeable cations, and the ion strength in the surrounding soil solution (Gruba and Mulder 2015). Consequently, changes in soil pH correspond to variations in soil surface charge, altering the distribution and mobility of charged substances on particle surfaces.

Previous research has shown that microbial inoculants can enhance nutrient cycling, plant root growth, and mineral dissolution (Warnock et al. 2007). Microorganisms affect soil particle surface charge density and specific surface area through the production and decomposition of organic matter and exudates, including organic acids, polysaccharides (Sauze et al. 2017). These compounds can bind to soil particles and increase their negatively charged compounds (Yukselen-Aksoy and Kaya 2010, Zhao et al. 2019) , impacting soil particle surface charge and specific surface area, ultimately enhancing soil CEC. Soil E_0 and φ_0 are determined by the distribution and density of charged substances on their surfaces. E_0 and φ_0 can influence soil aggregation by affecting the intensity of electrostatic forces between particles (Qafoku et al. 2004). High E_0 and φ_0 values promote aggregation by increasing the attractive forces between oppositely charged particles (Hu et al. 2015). The overall impact on soil aggregation depends on factors such as soil pH, ion strength, and the presence of organic matter, consistent with our structural equation model fitting results (Figure 4).

The wet sieving method, a simple and time-efficient technique for determining aggregate stability, was employed in this study, using the D (fractal dimension) as a comprehensive indicator of various aggregate sizes. Smaller D values indicate higher aggregate stability (Zeng et al. 2018). The application of rock-dissolving microbial inoculants improved the mass percentage of larger aggregates while reducing that of 0.053mm aggregates (Figure 2). Similar results were observed in sandy loam soils under intensive cultivation in the North China Plain after long-term application of microbial fertilizers (Wiesmeier et al. 2014) .As reported, the formation of micro-aggregates is promoted by the generation of multiple potential adsorption areas on clay particle surfaces, increasing soil ligands and cation exchange adsorption forces due to microbial surface charge (Ma et al. 2021). In previous studies, soil

aggregation has been attributed to the crossing or binding/wrapping effect of cover crop root networks (Sadeghi et al. 2017). However, root networks cannot act at nanometer distances of small soil particles (i.e., 2μm), and other factors must determine the interactions between small soil particles at the microscale. Research has shown that intrasoil forces (net forces) effectively control aggregate stability (Xu et al. 2014) and are closely related to soil particle electrochemical properties (Barber and Rowell 1972).

The Redundancy Analysis (RDA) and Structural Equation Modeling (SEM) were used to better understand the relationships among soil aggregate stability characteristics, soil physicochemical properties, and soil electrochemical properties. Our research results indicate that pH, clay content, soil CEC, and φ_0 are the key drivers affecting soil aggregate stability (Figure 4). Compared to other studies, our findings highlight the important role of these factors in soil aggregate stability. In previous research, microbial activity has been shown to influence pH values and soil colloidal properties (Yamagishi et al. 2017), while soil CEC is determined by colloidal surface characteristics (Totsche et al. 2018). Surface charges are generated through the dissociation or protonation of functional groups, which in turn affect the surface properties of soil colloids and consequently influence soil stability (Liu et al. 2014). Moreover, we founded that an increase in clay content may promote soil aggregate stability, which can be attributed to the adhesion of clay particles during the aggregation process (Huang 2004). The research findings on the role of soil electrochemical properties in soil aggregate stability provide new insights for a deeper understanding of the factors influencing soil aggregate stability.

Our findings have practical implications for the specific rock-dissolving microbial inoculants and vegetation restoration efforts we investigated. Applying rock-dissolving microbial inoculants can promote rock dissolution through organic acid secretion, thereby improving soil properties, enhancing soil electrochemical characteristics, and ultimately increasing soil aggregate stability. This is vital for the successful vegetation restoration and long-term ecosystem recovery of degraded mining areas. Future research should continue to explore these relationships across various soil types and environmental conditions to optimize soil management practices and promote ecosystem restoration.

7. Conclusion

In this study, we added exposed rock to the pot experiment and incorporated selected mineral-dissolving microbes into the external soil spray-seeding substrate, with the aim of improving the aggregate stability of the externally applied soil. The addition of microbes led to a decrease in soil pH, an increase in cation exchange capacity, and an increase in clay content. To some extent, the addition of microbes also increased the specific surface area and surface charge of soil particles, which directly influenced soil aggregate stability. Meanwhile, soil pH, cation exchange capacity, and clay content can both directly and indirectly affect soil aggregate stability.

In summary, our findings demonstrate the significant role of mineral-dissolving microbes in slope stability and contribute to a better understanding of the potential of mineral-dissolving microbes as a viable approach for ecological restoration. However, further research is needed to optimize the application of these microbes and assess their long-term impact on soil health and vegetation establishment in different mining environments.

Funding: This research was supported by the National Special Fund for Forestry Scientific Research of the Jiangsu Agriculture Science and Technology Innovation Fund (Grant No. CX (17)1004), the Natural Science Foundation for Youth of Jiangsu Province (BK20200785), and the Priority Academic Program Development of Jiangsu Higher Education Institutions (PAPD).

Data Availability Statement: The data presented in this study are available on request from the corresponding author.

Conflicts of Interest: The authors declare that they have no competing interests.

References

1. Abd Halin NI., Huyop F., Hamid THAT., Halim KBA, Hamid AAA., 2017. In silico binding interactions of dehalogenase (Dehe) with various haloalkanoic acids. Science Heritage Journal 1: 4-6.
2. Abd Samad NS., Amid A., Jimat DN., N. Ab. Shukor NA., 2017. Isolation and identification of halophilic bacteria producing halotolerant protease. Science Heritage Journal 1: 7-9.

3. Ali W., Hussain S., Chen J., Hu F., Liu J., He Y., Yang M., 2023. Cover crop root-derived organic carbon influences aggregate stability through soil internal forces in a clayey red soil. Geoderma 429: 116271.
4. Barber RG., Rowell DL., 1972. Charge distribution and the cation exchange capacity of an iron-rich kaolinitic soil. European Journal of Soil Science 23: 135-146.
5. Baumert VL., Vasilyeva NA., Vladimirov AA., Meier IC., Kögel-Knabner I., Mueller CW., 2018. Root exudates induce soil macroaggregation facilitated by fungi in subsoil. Frontiers in Environmental Science 6: 140.
6. Calero J., Ontiveros-Ortega A., Aranda V., Plaza I., 2017. Humic acid adsorption and its role in colloidal-scale aggregation determined with the zeta potential, surface free energy and the extended-DLVO theory. European Journal of Soil Science 68: 491-503.
7. Chaparro JM., Sheflin AM., Manter DK., Vivanco JM., 2012. Manipulating the soil microbiome to increase soil health and plant fertility. Biology and Fertility of Soils 48: 489-499.
8. Eddefli F., Ouakil A., Khaddari A., Tayebi M., 2023. Modeling Soil Erosion Using RUSLE and GIS–A Case Study of Korifla Sub-Watershed (Central Morocco). Ecological Engineering & Environmental Technology 24: 128-137.
9. Elliott ET., 1986. Aggregate structure and carbon, nitrogen, and phosphorus in native and cultivated soils. Soil Science Society of America Journal 50: 627-633.
10. Gruba P., Mulder J., 2015. Tree species affect cation exchange capacity (CEC) and cation binding properties of organic matter in acid forest soils. Science of The Total Environment 511:655-662.
11. GUERRA AJT., Fullen MA., JORGE MCO., BEZERRA JFR., Shokr MS., 2017. Slope processes, mass movement and soil erosion: A review. Pedosphere 27: 27-41.
12. Guimarães BM., Arends J., Van der Ha D., de Wiele TV., Boon N., Verstraete W., 2010. Microbial services and their management: recent progresses in soil bioremediation technology. Applied Social Ecology 46: 157-167.
13. Hepper EN., Buschiazzo DE., Hevia GG., Urioste A., Antón L., 2006. Clay mineralogy, cation exchange capacity and specific surface area of loess soils with different volcanic ash contents. Geoderma 135: 216-223.
14. Hu F., Xu C., Li H., Li S., Yu Z., Li Y., He X., 2015. Particles interaction forces and their effects

on soil aggregates breakdown. Soil and Tillage Research 147: 1-9.

15. Hu F., Xu C., Ma R., Tu K., Yang J., Zhao S., Yang M., Zhang F., 2021. Biochar application driven change in soil internal forces improves aggregate stability: Based on a two-year field study. Geoderma 403: 115276.
16. Hu W., Cheng WC., Wang L, Xue ZF., 2022. Micro-structural characteristics deterioration of intact loess under acid and saline solutions and resultant macro-mechanical properties. Soil and Tillage Research 220: 105382.
17. Huang PM., 2004. Soil mineral-organic matter-microorganism interactions: fundamentals and impacts. Advances in Agronomy 82: 393-472.
18. Iturri LA., Buschiazzo DE., 2014. Cation exchange capacity and mineralogy of loess soils with different amounts of volcanic ashes. CATENA 121: 81-87.
19. Jia Z., Meng M., Li C., Zhang B., Zhai L., Liu X., Ma S., Cheng X., Zhang J., 2021. Rock-Solubilizing Microbial Inoculums Have Enormous Potential as Ecological Remediation Agents to Promote Plant Growth. Forests 12: 357.
20. Jiang NJ., Tang CS., Yin LY., Xie YH., Shi B., 2019. Applicability of microbial calcification method for sandy-slope surface erosion control. Journal of Materials in Civil Engineering 31: 04019250.
21. Khan MS., Zaidi A., Wani PA., 2009. Role of phosphate solubilizing microorganisms in sustainable agriculture-a review. Agronomy for Sustainable Development 27: 29-43.
22. Kinnell PIA., 2005. Raindrop-impact-induced erosion processes and prediction: a review. Hydrological Processes 19: 2815-2844.
23. Li C., Jia Z., Ma S., Liu X., Zhang J., Müller C., 2023. Plant and native microorganisms amplify the positive effects of microbial inoculant. Microorganisms 11: 570.
24. Li C., Jia Z., Yuan Y., Cheng X., Shi J., Tang X., Wang Y., Peng X., Dong Y., Ma S., Li Q., Liu X., Chen J., Zhang J., 2020. Effects of mineral-solubilizing microbial strains on the mechanical responses of roots and root-reinforced soil in external-soil spray seeding substrate. Science of The Total Environment 723: 138079.
25. Li C., Jia Z., Zhai L., Zhang B., Peng X., Liu X., Zhang J., 2021. Effects of Mineral-Solubilizing Microorganisms on Root Growth, Soil Nutrient Content, and Enzyme Activities in the Rhizosphere

Soil of Robinia pseudoacacia. Forests 12: 60.

26. Li H., Hou J., Liu X., Li R., Zhu H., Wu L., 2011. Combined Determination of Specific Surface Area and Surface Charge Properties of Charged Particles from a Single Experiment. Soil Science Society of America Journal 75: 2128-2135.
27. Li S., Li Y., Shi J., Zhao T., Yang J., 2017. Optimizing the formulation of external-soil spray seeding with sludge using the orthogonal test method for slope ecological protection. Ecological Engineering 102: 527-535.
28. Liu J., Hu F., Xu C., Wang Z., Ma R., Zhao S., Liu G., 2021. Comparison of different methods for assessing effects of soil interparticle forces on aggregate stability. Geoderma 385:114834.
29. Liu J., Wang Z., Hu F., Xu C., Ma R., Zhao S., 2020. Soil organic matter and silt contents determine soil particle surface electrochemical properties across a long-term natural restoration grassland. CATENA 190: 104526.
30. Liu J., Yang Y., Zheng Q., Su X., Liu J., Zhou Z., 2022. Effects of soil surface electrochemical properties on soil detachment regulated by soil types and plants. Science of The Total Environment 834:154991.
31. Liu X., Li H., Li R., Tian R., Xu C., 2013. Combined determination of surface properties of nano-colloidal particles through ion selective electrodes with potentiometer. Analyst 138: 1122-1129.
32. Liu X., Li H., Li R., Xie D., Ni J., Wu L., 2014. Strong non-classical induction forces in ion-surface interactions: General origin of Hofmeister effects. Scientific Reports 4: 5047.
33. Ma R., Hu F., Liu J., Zhao S., 2021. Evaluating the effect of soil internal forces on the stability of natural soil aggregates during vegetation restoration. Journal of Soils and Sediments 21: 3034-3043.
34. Ma R., Hu F., Xu C., Liu J., Yu Z., Liu G., Zhao S., Zheng F., 2023. Vegetation restoration enhances soil erosion resistance through decreasing the net repulsive force between soil particles. CATENA 226: 107085.
35. Meng J., Li XA., 2019. Effects of carbonate on the structure and properties of loess and the corresponding mechanism: an experimental study of the Malan loess, Xi'an area, China. Bulletin of Engineering Geology and the Environment 8: 4965-4976.

36. O'Donnell ST., Kavazanjian E., Rittmann BE., 2017. MIDP: Liquefaction mitigation via microbial denitrification as a two-stage process. II: MICP. Journal of Geotechnical and Geoenvironmental Engineering 143: 04017095.
37. Prabhakaran P., Ashraf MA., Aqma WS., 2016. Microbial stress response to heavy metals in the environment. RSC Advances 6: 109862-109877.
38. Qafoku NP., Ranst EV., Noble AD., Baert G., 2004. Variable charge soils: their mineralogy, chemistry and management. Advances in Agronomy 84: 159-215.
39. Rengasamy P., Olsson KA. 1991. Sodicity and soil structure. Australian Journal of Soil Research 29: 935-952.
40. Sadeghi SH., Harchegani MK., Asadi H., 2017. Variability of particle size distributions of upward/downward splashed materials in different rainfall intensities and slopes. Geoderma 290: 100-106.
41. Safar F., Whalen JK., 2023. Mechanical stability of newly-formed soil macroaggregates influenced by calcium concentration and the calcium counter-anion. Geoderma 430: 116333.
42. Sauze J., Ogée J., Maron PA., Crouzet O., Nowak V., Wohl S., Kaisermann A., Jones SP., Wingate L., 2017. The interaction of soil phototrophs and fungi with pH and their impact on soil CO2, CO18O and OCS exchange. Soil Biology and Biochemistry 115: 371-382.
43. Soil Survey Staff., 2014. Keys to soil taxonomy.
44. Totsche KU., Amelung W., Gerzabek MH., Guggenberger G., Klumpp E., Knief C., Lehndorff E., Mikutta R., Peth S., Prechtel A., Ray N., Kogel-Knabner I., 2017. Microaggregates in soils. Journal of Plant Nutrition and Soil Science 181:104-136.
45. Wang G., Deng H., Nie L., Wu Y., Zhang J., 2018. Mechanism of limestone corrosion by Gongronella butleri NL-15. Applied Environmental Biology 24:374-378.
46. Wang J., Fu Z., Ren Q., Zhu L., Lin J., Zhang J., Cheng X., Ma J., Yue J., 2019. Effects of arbuscular mycorrhizal fungi on growth, photosynthesis, and nutrient uptake of Zelkova serrata (Thunb.) Makino seedlings under salt stress. Forests 10:186.
47. Wang YX., Zhang JC., Wu YW., Wang JL., Jia ZH., 2017. Effects of soil bacteria inoculation in spray seeding matrix on photosynthesis characteristics and chlorophyll fluorescence parameters of Amorpha fruticose. Research of Environmental Sciences 30: 902-910.

48. Warnock DD., Lehmann J., Kuyper TW., Rillig MC., 2007. Mycorrhizal responses to biochar in soil–concepts and mechanisms. Plant and Soil 300: 9-20.
49. Wei J., Shi B., Li J., Li S., He X., 2018. Shear strength of purple soil bunds under different soil water contents and dry densities: A case study in the Three Gorges Reservoir Area, China. 166: 124-133.
50. Wiesmeier M., Hübner R., Spörlein P., Geuß U., Hangen E., Reischl A., Schilling B., von Lützow M., Kögel-Knabner I., 2014. Carbon sequestration potential of soils in southeast Germany derived from stable soil organic carbon saturation. Global Change Biology 20: 653-665.
51. Wu F., Luo Y., Chang Z., 2011. Slope reinforcement for housing in Three Gorges reservoir area. Journal of Mountain Science 8: 314-320.
52. Wu Yw., Zhang Jc., Wang Lj., Wang Yx., 2017a. A rock-weathering bacterium isolated from rock surface and its role in ecological restoration on exposed carbonate rocks. Ecological Engineering 101: 162-169.
53. Wu Y., Zhang J., Guo X., Wang Y., Wang Q., 2017b. Isolation and characterisation of a rock solubilising fungus for application in mine-spoil reclamation. European Journal of Soil Biology 81: 76-82.
54. Wu Y., Zhang J., Guo X., 2017. An indigenous soil bacterium facilitates the mitigation of rocky desertification in carbonate mining areas. Land Degradation & Development 28: 2222-2233.
55. Xu H., Li TB., Chen JN., Liu CN., Xh Zhou., Xia L., 2017. Characteristics and applications of ecological soil substrate for rocky slope vegetation in cold and high-altitude areas. Science of The Total Environment 609: 446-455.
56. Xu R., Li J., Jiang J., 2014. Progresses in research on special chemical phenomena and their mechanisms in variable charge soils. Acta Pedologica Sinica 51: 207-215.
57. Yamagishi K., Kizaki K., Ito S., Hirata R., Mitsuda Y., 2017. Effect of surface soil conservation by litter from shelterbelts on Chamaecyparis obtusa plantation. Environmental Sciences 22: 69-73.
58. Yukselen-Aksoy Y., Kaya A., 2010. Method dependency of relationships between specific surface area and soil physicochemical properties. Applied Clay Science 50: 182-190.
59. Zeng Q., Darboux F., Man C., Zhu Z., An S., 2018. Soil aggregate stability under different rain conditions for three vegetation types on the Loess Plateau (China). CATENA 167: 276-283.

60. Zhao B., Liu X., Xia D., Liu D., Xia Z., Xu W., Zhao J., 2018. Effect of Cement Content in Vegetation Concrete on Soil Physico-chemical Properties, Enzyme Activities and Microbial Biomass. Nature Environment and Pollution Technology 17: 1065-1075.
61. Zhao Z., Chang E., Lai P., Dong Y., Xu R., Fang D., Jiang J., 2019. Evolution of soil surface charge in a chronosequence of paddy soil derived from Alfisol. Soil and Tillage Research 192: 144-150.
62. Zhu X., Chen H., Li W., He Y., Brookes PC., Xu J., 2014. Aggregation kinetics of natural soil nanoparticles in different electrolytes. European Journal of Soil Science 65: 206-217.